Search for supersymmetry in two photon + jet events in pp collisions at $\sqrt{s} = 8$

with a brief discussion:

Motivation and trigger strategies for displaced jet searches in LHC Run 2 data

Joshua Hardenbrook - Princeton University

November 23nd, 2014

In Fullfillment of the Princeton Physics PhD Pre-Thesis Requirement

Advisor: Professor Christopher Tully

Abstract:

A search for supersymmetry in pp collisions, in events with at least two photons and one jet, is presented. The dataset, collected at a center-of-mass energy $\sqrt{s} = 8$ TeV in 2012, corresponds to an integrated luminosity of 19.7 fb^{-1}. The signal is characterized as a peak on a falling background in the razor kinematic variable $\mathrm{M_R}$, for events in the tail of the razor ratio R^2. The observed event distribution in $\mathrm{M_R}$ is compatible with the prediction derived by the events with small values of R^2. This result is interpreted as an exclusion limit on a set of simplified model spectra for squarks and gluinos, inspired by the phenomenology of gauge-mediated supersymmetry breaking.

Additionally, the prospects for displaced jet searches will be discussed. Current triggering algorithms will be outlined as well as possible discovery motivated analysis strategies.

1 Introduction

The existence of supersymmetry (SUSY) [1–9] at the electro-weak energy scale is postulated to extend the standard model (SM) of particle physics, such that the mass of the lightest Higgs boson is stabilized, canceling the divergent quantum corrections from fermionic loops with the equivalent contributions from bosonic super partners, and vice versa. Assuming R-parity conservation, only even numbers of SUSY particles can be produced at particle accelerators, the lightest SUSY partner (LSP) being stable. SUSY must be a broken symmetry since SUSY partners degenerate with SM particles have not been observed. Among the several SUSY breaking mechanisms proposed, General Gauge Mediated (GGM) supersymmetry breaking [10–18] provides an interesting phenomenology for proton-proton collisions at the Large Hadron Collider (LHC). In particular, many GGM models predict that the gravitino $\widetilde{\mathrm{G}}$ and the neutralino $\widetilde{\chi}$ are the LSP and the next-to-lightest supersymmetric particle (NLSP), respectively.

In this note, we concentrate on final states containing at least two prompt photons and one jet, originating from the cascade decay of squarks and gluinos to a pair of $\widetilde{\chi}$ and jets, with $\widetilde{\chi}$ decaying to $\widetilde{\mathrm{G}}\gamma$. The events will also have missing transverse energy ($E_{\mathrm{T}}^{\mathrm{miss}}$) due to the LSP $\widetilde{\mathrm{G}}$. We consider pp collisions collected by the Compact Muon Solenoid (CMS) detector at the LHC in 2012, at a center-of-mass energy $\sqrt{s} = 8\,\mathrm{TeV}$. The dataset presented here corresponds to an integrated luminosity of $L = 19.7\ \mathrm{fb}^{-1}$.

In a previous CMS study [19], this SUSY signature was searched for by studying events with large $E_{\mathrm{T}}^{\mathrm{miss}}$ in $4.0\,\mathrm{fb}^{-1}$ of $\sqrt{s} = 8\,\mathrm{TeV}$ data. No evidence for a signal was found and GGM models with production cross section larger than $\approx 10\ \mathrm{fb}^{-1}$ were excluded. A more recent ATLAS study searching for GGM SUSY signatures in two-photon+$E_{\mathrm{T}}^{\mathrm{miss}}$ events in $20.3\,\mathrm{fb}^{-1}$ of $\sqrt{s} = 8\,\mathrm{TeV}$ data set lower limits on gluino and wino masses of 1280 GeV and 570 GeV, respectively, for bino masses above 50 GeV [20].

In this updated study, the two-photon+jet+$E_{\mathrm{T}}^{\mathrm{miss}}$ topology is investigated in a purely data-driven way using the razor variables [21, 22] $\mathrm{M_R}$ and R^2, characterizing the signal as a wide excess in $\mathrm{M_R}$ emerging above the falling SM background, for events populating the tail of the R^2 distribution. The background $\mathrm{M_R}$ shape is determined in a control region of the ($\mathrm{M_R}$, R^2) plane and extrapolated to the tail of R^2. This data-driven background estimate is tested on a control sample of events with calorimetric deposits from hadrons, misidentified as photons. By using R^2, it is possible to extend the study in Ref. [19], accessing events with large R^2 but lower $E_{\mathrm{T}}^{\mathrm{miss}}$.

The observed data distribution in the signal region is found to be in agreement with the predicted background distribution. The result is interpreted in a set of simplified model spectra (SMS) [23–26], inspired by the GGM models.

2 Event selection

The events selected in this study are required to have at least one high-quality reconstructed interaction vertex. If more than one vertex is found, the one with the highest associated $\sum_{\mathrm{track}} p_{\mathrm{T}}^2$, where p_{T} is transverse momentum, is selected and used in the global event reconstruction. A set of detector- and beam-related cleaning algorithms is applied to remove events with detector noise, which would fake signal-like events with high energy and large $E_{\mathrm{T}}^{\mathrm{miss}}$.

Events are collected using the resonant and non-resonant triggers utilized by the higgs to two photon analysis [27]. The triggers use complementary photon selections. One selection requires a loose calorimetric identification based on the shape of the electromagnetic shower and loose isolation requirements on the photon candidates, while the other requires only that the photon have a high value of the shower shape variable R_9. The photons are required to have transverse energy of 26 (18) GeV and 36 (22) GeV on the leading (trailing) photon for the resonant and non-resonant trigger respectively. The effect of the mass cut on non-resonant photons in the intermediate range is found to be less than 1 percent for the targeted signals.

The event reconstruction is performed using the particle flow (PF) algorithm [28], which combines the information of the various detector components in a coherent view of the detected process. Individual particles are reconstructed and classified in five categories: muons, electrons, photons, charged hadrons, and neutral hadrons.

Photons are identified applying a set of loose requirements on isolation and energy cluster shape [29]. At least two photons are required in the event, the highest-p_{T} (second highest-p_{T}) photon having $p_{\mathrm{T}} > 30$ (22) GeV. Photons are also required to be within the fiducial region of the tracker ($|\eta| < 2.5$).

The reconstructed PF candidates are clustered using the anti-$\mathrm{k_T}$ [30] algorithm, with jet size set to $R = 0.5$, using FASTJET [31]. Jets are selected with $p_{\mathrm{T}} > 40$ GeV and $|\eta| < 2.5$, with each jet required to have a distance $\Delta R = \sqrt{(\Delta\eta)^2 + (\Delta\phi)^2} > 0.5$ from each identified photon. In order to remove jets due to detector noise, jets are required to have at least two constituents. In addition, the fraction of transverse momentum associated with each PF-candidate category (hadronic, neutral hadronic, etc) is required to be < 0.99. At least one jet passing the above criteria is required in each event.

3 Analysis strategy

The razor approach to SUSY event reconstruction aims to approximate the rest frame of the pair-produced SUSY partners. The razor variables were proposed to describe the two-jet topology resulting from the production of two squarks, each decaying to a quark and the LSP, assumed to be a stable neutralino $\widetilde{\chi}^0_1$ [21, 22].

Given a two-jet event, $\mathrm{M_R}$ is defined as:

$$\mathrm{M_R} \equiv \sqrt{(|\vec{p}_{\mathrm{j_1}}| + |\vec{p}_{\mathrm{j_2}}|)^2 - (p_z^{\mathrm{j_1}} + p_z^{\mathrm{j_2}})^2}\,, \tag{1}$$

where $\vec{p}_{\mathrm{j}_i}$, $\vec{p}_{\mathrm{T}}^{\,\mathrm{j}_i}$, and $p_z^{\mathrm{j}_i}$ are the momentum of the ith-jet, its transverse component, and its longitudinal component, respectively. The transverse momentum imbalance in the event is quantified by the variable $\mathrm{M_T^R}$, defined as

$$\mathrm{M_T^R} \equiv \sqrt{\frac{\mathrm{E_T^{miss}}(p_{\mathrm{T}}^{\mathrm{j_1}} + p_{\mathrm{T}}^{\mathrm{j_2}}) - \vec{\mathrm{E}}_{\mathrm{T}}^{\mathrm{miss}} \cdot (\vec{p}_{\mathrm{T}}^{\,\mathrm{j_1}} + \vec{p}_{\mathrm{T}}^{\,\mathrm{j_2}})}{2}}\,, \tag{2}$$

where $\mathrm{E_T^{miss}}$ and pt_i^{j} are the magnitude of $\vec{\mathrm{E}}_{\mathrm{T}}^{\mathrm{miss}}$ and $\vec{p}_{\mathrm{T}}^{\,\mathrm{j}_i}$, respectively. For $\widetilde{\mathrm{q}}$ pair production with $\widetilde{\mathrm{q}} \to \widetilde{\chi}^0_1\mathrm{q}$, the distribution of $\mathrm{M_R}$ peaks at

$$\mathrm{M}_\Delta = (m_{\widetilde{\mathrm{q}}}^2 - m_{\widetilde{\chi}^0_1}^2)/m_{\widetilde{\mathrm{q}}}\,, \tag{3}$$

where m_{p} is the mass of a particle p. For the same events, $\mathrm{M_T^R}$ has a kinematic edge at M_Δ. The razor ratio R is defined as

$$\mathrm{R} \equiv \frac{\mathrm{M_T^R}}{\mathrm{M_R}}\,. \tag{4}$$

For longer decay chains, as those considered in this study, the M_R distribution becomes wider, but the qualitative features of the M_R and R are retained.

In order to compute the values of M_R and R for generic two-photon+jets+E_T^{miss} events, we consider the set of reconstructed jets and photons in the event. The items of this set are grouped in two exclusive groups, referred to as "megajets". The four-momentum of a megajet is computed as the vectorial sum of the four-momenta of its constituents. Among all the possible megajet pairs in an event, we select the megajet pair with the smallest sum of squared invariant masses. Although the two photons of the event are not explicitly required to be in different megajets, they are nonetheless predominantly placed in opposite megajets. For the samples considered, the photons are always placed in opposite megajets in more than 80 % of events depending on the specific model point with a mode of 99 % (86%) for the T5gg (GGM) samples. It is found that when the photons are not placed in opposite hemispheres, the corresponding change in M_R is at most 15%. Isolated leptons which pass the jet identification criteria can enter the hemisphere clustering as jets. Events with isolated leptons failing the jet identification criteria are clustered without including the jet associated with the lepton. Additionally, all jets are required to be well separated from the two photons to be included in the clustering.

The (M_R, R^2) plane is divided in two different regions: i) a signal region, containing events with $M_R > 600$ GeV and $R^2 > 0.02$; ii) a control region, defined by requiring $M_R > 600$ GeV and $0.01 < R^2 \leq 0.02$. The control region is defined such that any potential signal contamination is less than 10% of the expected number of signal events ($\sigma \times L$) and thus has a negligible bias on the determination of the background shape which is at worst 1-2% for a signal of size $\sigma \times L \approx 20$.

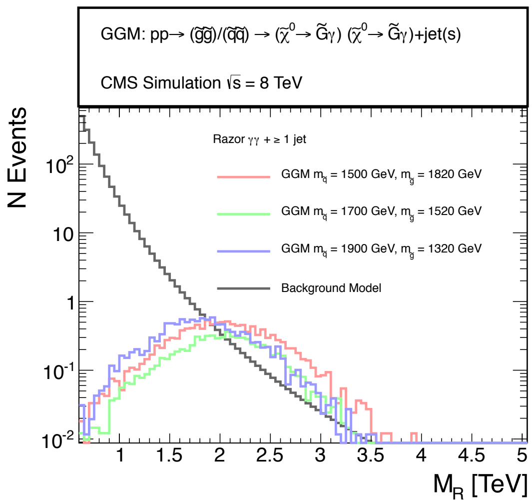

(a)

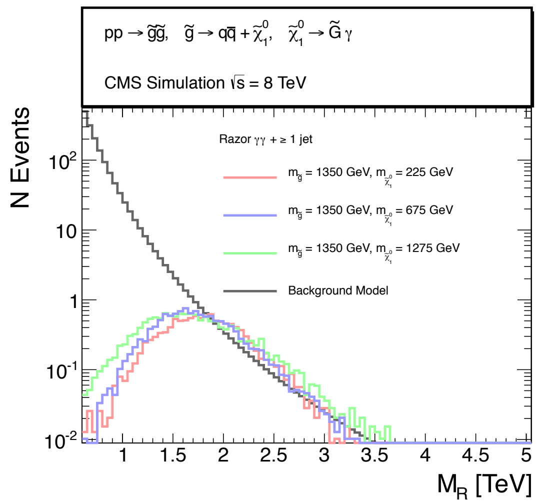

(b)

Figure 1: Signal vs. Background distributions in M_R for the two interpretations: (a) squark-gluino model (b) T5gg model. The background model is normalized to the number of events in the signal region. The signal points are normalized to integrated luminosity times selection efficiency times theoretical cross section.

4 Background prediction and validation

A maximum likelihood fit of the M_R data distribution in the control region is performed, using the functional form

$$P(M_R) \propto e^{-k(M_R - M_R^0)^{\frac{1}{n}}} \quad (5)$$

where M_R^0 is an offset parameter, k quantifies the slope of the 1D distribution in the exponential limit and n describes a deviation from an exponential fall. The parameters obtained are used to describe M_R in the signal region, fixing the overall normalization of the control region fit to the observed yield in the signal region. The covariance matrix derived from the fit in the control region is derived to sample an ensemble of alternative M_R background shapes. For each bin of the M_R distribution, a probability distribution for the yield is derived. A 68% probability range is computed for each yield distribution, using the probability density as ordering principle.

The method is tested using a control sample of jets misidentified as photons, obtained by selecting photon candidates which fail the cluster-shape selection or the isolation requirement, while keeping the rest of the photon selection unaltered (fake-fake sample). In Fig 2 (a) and (b) we show the fit result in the control region and the extrapolation to the signal region, respectively. From previous studies [22], one would expect the M_R shapes in the control region and the signal region to be different, due to the different lower threshold applied to define the two regions. These tests shows that the choice of using a narrow control region makes the distortion of the M_R distribution negligible. The influence of potential backgrounds with real E_T^{miss} (such as $t\bar{t}$ or $W\gamma$) on the method has been investigated using simulation and has been found to be small and well contained within the systematic uncertainty assigned to the method.

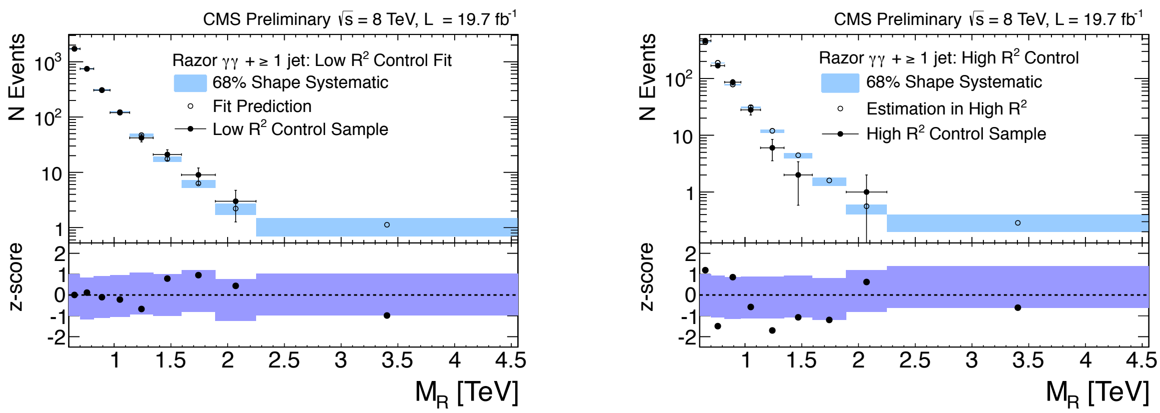

(a) (b)

Figure 2: Data distribution for M_R in the fake-fake control sample (a) in the control region and (b) in the signal region. For each M_R bin, the data (filled dots) are compared to the 68% range obtained from the fit in the control region and extrapolated to the signal region, represented by the blue outlined band. The empty dots represent the center of the 68% range. The bottom panel of each figure gives the z-score (number of gaussian standard deviations) comparing the filled dots to the band. The purple band shows the position of the 68% window about the expected value.

A signal originating from heavy squarks or gluinos would result in an wide bump emerging in the M_R distribution. This is shown in Fig. 3, where a signal sample of squarks and gluinos, with masses set respectively to $m_{\tilde{q}} = 1400$ GeV and $m_{\tilde{g}} = 1820$ GeV and the production cross section $\sigma = 2.7$ fb, is added to the fake-fake sample. The signal contamination is negligible in the control region and it does not change the background shape of Fig. 2 (a). On the other hand, the extrapolation would not account for the excess in the tail in the presence of signal.

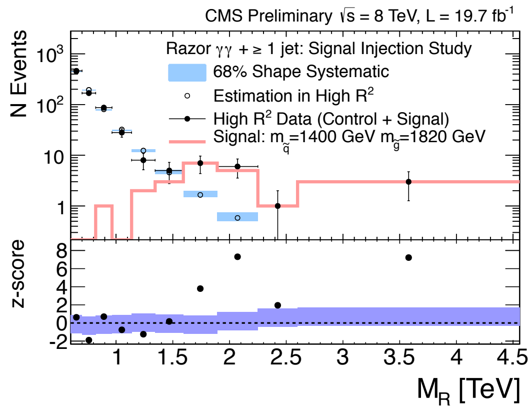

Figure 3: Data distribution for M_R in a sample of fake-fake data events and injected with simulated squark and gluino events. Squark and gluino masses are set to $m_{\tilde{q}} = 1400$ GeV and $m_{\tilde{g}} = 1820$ GeV respectively, and the production cross section is fixed to $\sigma = 2.7$ fb. The signal contribution is shown by the red histogram. For each M_R bin, the data (filled dots) are compared to the 68% range obtained from the fit in the control region and extrapolated to the signal region, represented by the blue outlined band. The empty dots represent the center of the 68% range. The bottom panel of each figure gives the z-score (number of gaussian standard deviations) comparing the filled dots to the band. The purple band shows the position of the 68% window about the expected value. .

5 Systematic uncertainty

The systematic uncertainty in the background data-driven method originates from the fit uncertainty in the control region. The uncertainty is quantified in each M_R bin from the yield distribution derived from an ensemble of background shapes, sampled from the fit covariance matrix. The jet energy corrections contribute to the systematic uncertainty on the signal distribution. The knowledge of the parton density functions and the integrated luminosity contribute to the uncertainty on the signal normalization.

The typical size of each contribution is summarized in Table 1. The shape systematics on the background are determined bin by bin with smaller systematics where the fit shape is constrained (in lower M_R bins) , and larger where uncertainy in the fit parameters accomodate larger deviations in the expected number of events (higher M_R bins). The percentage listed is to be interpreted as the fractional value of the expectation equivalent to a single guassian standard deviation. The fit shape systematic corresponds to uncertainty in the parameters in the fit. The fit function systematic estimates our uncertainty due to the choice of fit function and the differences between the control and signal region functional form. The background systematics dominante the uncertainty for the cross section upper limit interpretation.

The systematics on the signal are subdominant and are determined bin by bin if listed as shape. Systematics not listed as shape are flatly applied to the signal normalization (luminosity, trigger efficiency, signal rate, acceptance). Photon MC/Data systematics are applied to correct for known differences between the MC and Data event by event. Jet energy scale correction systematics apply to number of events in a given M_R bin. By varying the jet energy scale we

Background systematic	Value
Fit shape	shape (bin by bin) 4 - 40%
Fit function systematic	shape (bin by bin) 5 - 50%

Signal systematic	Value
Data/MC photon scale factors	1-2%
Trigger efficiency	1%
Luminosity	2.6%
Jet energy scale corrections	shape (bin by bin) 2-5%

Signal Specific Systematics	Squark-Gluino	T5gg
Acceptance due to PDF	1-3%	1%
Signal rate due to PDF	1.0 - 50%	included in SMS xsec error

Table 1: Typical size of the signal and background systematic uncertainties on shape and normalization.

induce a change in the shape of the signal M_R resonance. The percent listed corresponds to the percentage change in the M_R expectation due to a 1 guassian standard deviation modification up or down in the jet energy scale.

6 Results

The background-prediction method described in Section 4 is applied to the events selected by the requirements described in Section 2. Figure 4 (a) shows the fit output and the associated uncertainty band, compared to the data in the control region. The fit result is then used to derive the background prediction in the signal region. The comparison of the prediction to the observed data distribution is shown in Figure 4 (b). No evidence for a signal is found. The largest positive and negative deviation from the predictions are observed for $M_R \approx 2.3$ TeV and $1.1 \lesssim M_R \lesssim 1.9$ TeV, respectively, each corresponding to a local significance of ≈ 1.5 standard deviations.

7 Interpretation

The result is interpreted in two GGM-inspired SMS scenarios:

- **Squark-gluino model:** squark and gluino production including all flavors except the right-handed up-type, with the $\widetilde{\chi}_1^0$ mass fixed at 375 GeV. The $\widetilde{\chi}_1^0 \to \widetilde{G}\gamma$ decay occurs with branching ratio 100%. All other SUSY particles are decoupled with masses set to 5 TeV.
- **Simplified model T5gg:** gluino pair-production, with gluinos decaying to $q\bar{q}\widetilde{\chi}_1^0$, and $\widetilde{\chi}_1^0 \to \widetilde{G}\gamma$. All decays occur with branching ratio 100%.

In both models the gravitino mass is negligibly small ≈ 1 GeV. The corresponding Feynman diagrams for gluino-gluino and squark-squark production are shown in Fig. 5.

Events for T5gg are generated with MADGRAPH V5, in association with up to two partons. The SUSY particles are decayed in PYTHIA6 assuming a flat matrix element. The event is showered in PYTHIA6 and matched to the matrix-element kinematic configuration using the MLM

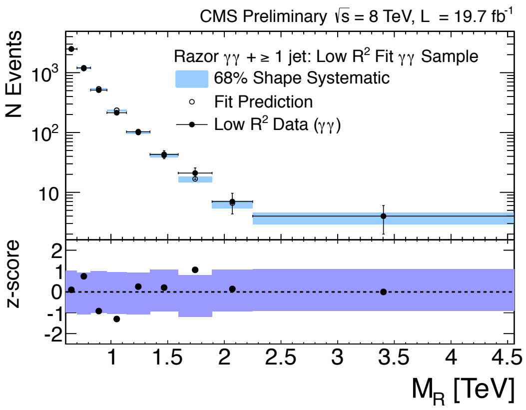

(a)

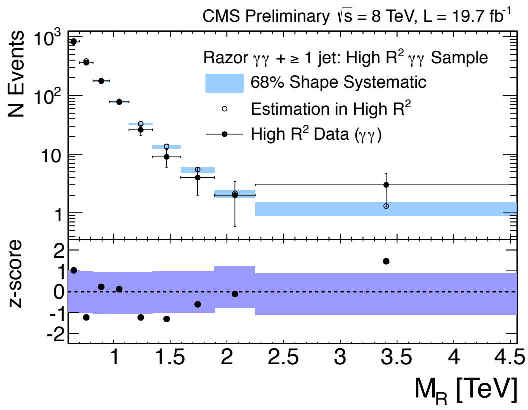

(b)

Figure 4: Data distribution for M_R in the data (a) control region and (b) signal region. For each M_R bin, the data (filled dots) are compared to the 68% range obtained from the fit in the control region and extrapolated to the signal region, represented by the colored band. The empty dots represent the center of the 68% range. The bottom panel of each figure gives the z-score obtained comparing the filled dots to the band. The purple band shows the position of the 68% window about the expected value.

algorithm [32] before being processed through a fast simulation of the CMS detector [33]. The gluino production production cross sections for T5gg is calculated to NLO and next-to-leading-logarithm (NLL) accuracy [34–38], assuming the decoupling of the other SUSY partners. The NLO+NLL cross section and the associated theoretical uncertainty [39] are taken as a reference to derive exclusion limits on SUSY particle masses. The corresponding information for the squark-gluino model is given in Ref. [19].

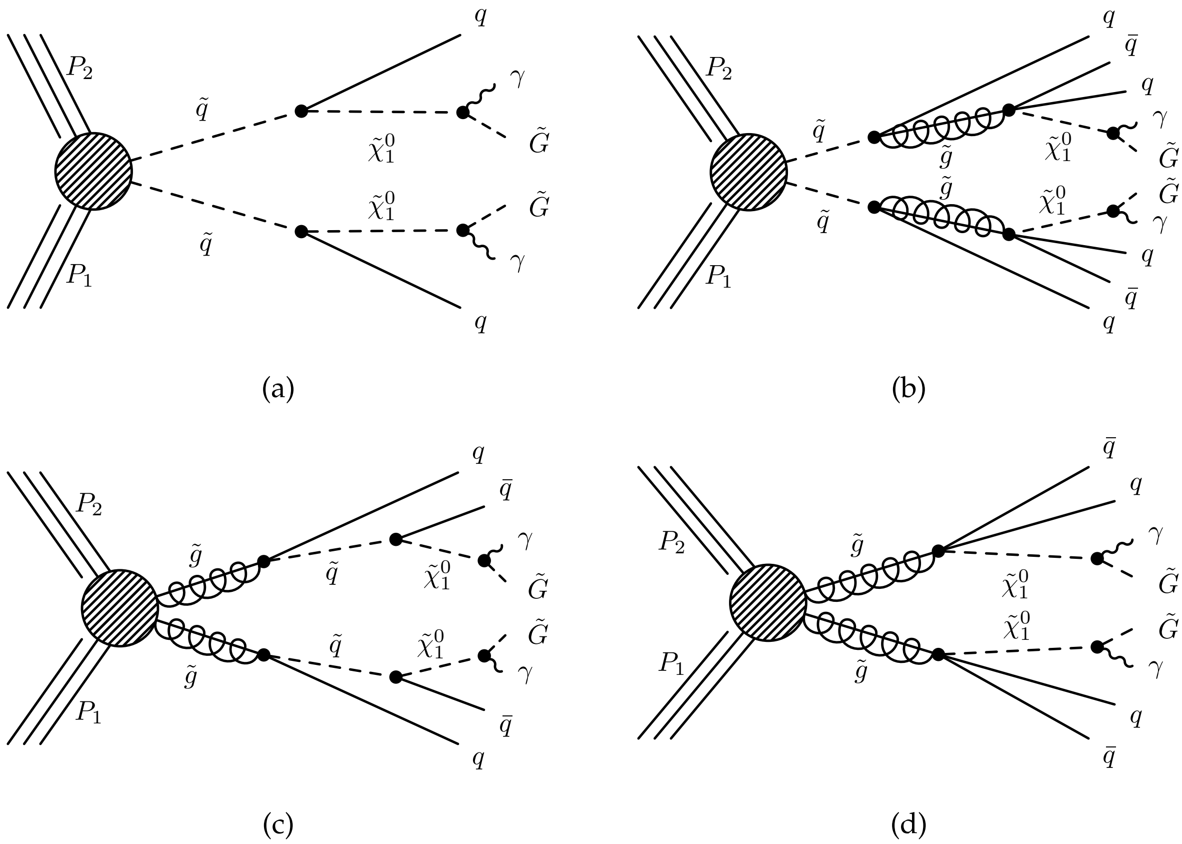

Figure 5: Feynman diagram for (a) squark-squark production, (b) squark-squark decaying through gluino-gluino, and (c) gluino-gluino decaying through squark-squark in the squark-gluino model and (d) for gluino-gluino in the simplified model T5gg.

In order to derive a limit on a given SUSY model, we use the LHC CL_s procedure [40]. The signal plus background likelihood function is defined by adding the signal comonent to the background component. Additional systematic effects to the normalization and the shape are modeled as log-normal systematics. The dependence of the likelihood on the nuisance parameters is removed through profiling. The ratio of the profiled likelihoods for the two hypotheses (σ fixed to the value under test versus $\hat{\sigma}$ obtained by maximizing the likelhiood, with $0 < \hat{\sigma} < \sigma$) is used as the test statistic to associate a CL_s value to each value of σ.

Fig 6 shows the excluded region in the ($m_{\tilde{\mathrm{g}}}$, $m_{\tilde{\mathrm{q}}}$) plane for the squark-gluino model, and the ($m_{\tilde{\mathrm{g}}}$, $\tilde{\chi}^0_1$) plane for T5gg. The red (black) dashed line shows the expected (observed) limit. The thin dashed line and band show the 68% range about the expected limit. The solid line quantifies the impact of the theoretical uncertainty in the cross section on the observed limit. The color code of the temperature plot shows the excluded cross section for each set of mass values.

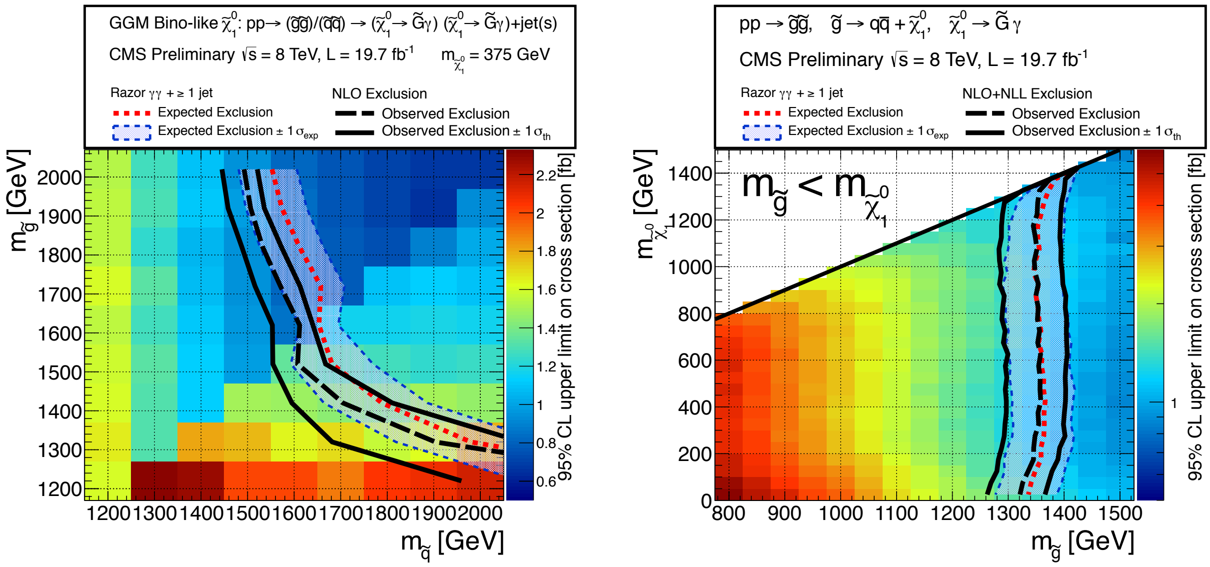

(a) (b)

Figure 6: Excluded mass region for (a) squark-gluino model and (b) T5gg. The red (black) dashed line shows the expected (observed) limit. The thin dashed blue line and band show the 68% range about the expected limit. The black solid line quantifies the impact of the theoretical uncertainty in the cross section on the observed limit. The color code to the right of the figure shows the excluded cross section for each set of mass values.

8 Conclusions

A search for supersymmetry in events with at least two photons and at least one jet is performed on pp collisions at $\sqrt{s} = 8$ TeV. The signal is characterized as as a wide bump in the distribution of the razor kinematic variable M_R, for events with large values of the razor ratio R^2. The signal is determined in a control region at low R^2 and extrapolated in the signal region. No excess is observed. The result is interpreted in terms of exclusion limits on squark and gluinos in GGM-inspired SMS. For comparable parameter space between the GGM and T5gg SMS, the T5gg SMS has a lower expected upper limit due to the 100 % branching fraction of the neutralino decay.

References

[1] J. Wess and B. Zumino, “Supergauge Transformations in Four-Dimensions”, *Nucl. Phys. B* **70** (1974) 39, doi:10.1016/0550-3213(74)90355-1.

[2] Y. Golfand and E. Likhtman, “Extension of the Algebra of Poincare Group Generators and Violation of p Invariance”, *JETP Lett.* **13** (1971) 323.

[3] D. Volkov and V. Akulov, “Possible universal neutrino interaction”, *JETP Lett.* **16** (1972) 438.

[4] A. H. Chamseddine, R. L. Arnowitt, and P. Nath, “Locally supersymmetric grand unification”, *Phys. Rev. Lett.* **49** (1982) 970, doi:10.1103/PhysRevLett.49.970.

[5] G. L. Kane, C. F. Kolda, L. Roszkowski, and J. D. Wells, "Study of constrained minimal supersymmetry", *Phys. Rev. D* **49** (1994) 6173, doi:10.1103/PhysRevD.49.6173, arXiv:hep-ph/9312272.

[6] P. Fayet, "Supergauge invariant extension of the Higgs mechanism and a model for the electron and its neutrino", *Nucl. Phys. B* **90** (1975) 104, doi:10.1016/0550-3213(75)90636-7.

[7] R. Barbieri, S. Ferrara, and C. A. Savoy, "Gauge models with spontaneously broken local supersymmetry", *Phys. Lett. B* **119** (1982) 343, doi:10.1016/0370-2693(82)90685-2.

[8] L. J. Hall, J. D. Lykken, and S. Weinberg, "Supergravity as the messenger of supersymmetry breaking", *Phys. Rev. D* **27** (1983) 2359, doi:10.1103/PhysRevD.27.2359.

[9] P. Ramond, "Dual theory for free fermions", *Phys. Rev. D* **3** (1971) 2415, doi:10.1103/PhysRevD.3.2415.

[10] P. Fayet, "Mixing Between Gravitational and Weak Interactions Through the Massive Gravitino", *Phys. Lett.* **B70** (1977) 461, doi:10.1016/0370-2693(77)90414-2.

[11] H. Baer, M. Brhlik, C. H. Chen, and X. Tata, "Signals for the Minimal Gauge-Mediated Supersymmetry Breaking Model at the Fermilab Tevatron Collider", *Phys. Rev.* **D55** (1997) 4463, doi:10.1103/PhysRevD.55.4463.

[12] H. Baer, P. G. Mercadante, X. Tata, and Y. L. Wang, "Reach of Tevatron Upgrades in Gauge-Mediated Supersymmetry Breaking Models", *Phys. Rev.* **D60** (1999) 055001, doi:10.1103/PhysRevD.60.055001.

[13] S. Dimopoulos, S. Thomas, and J. D. Wells, "Sparticle Spectroscopy and Electroweak Symmetry Breaking with Gauge-Mediated Supersymmetry Breaking", *Nucl. Phys.* **B488** (1997) 39, doi:10.1016/S0550-3213(97)00030-8.

[14] J. R. Ellis, J. L. Lopez, and D. V. Nanopoulos, "Analysis of LEP Constraints on Supersymmetric Models with a Light Gravitino", *Phys. Lett.* **B394** (1997) 354, doi:10.1016/S0370-2693(97)00019-1.

[15] M. Dine, A. Nelson, Y. Nir, and Y. Shirman, "New Tools for Low Energy Dynamical Supersymmetry Breaking", *Phys. Rev.* **D53** (1996) 2658, doi:10.1103/PhysRevD.53.2658.

[16] G. F. Giudice and R. Rattazzi, "Gauge-Mediated Supersymmetry Breaking", in *Perspectives on Supersymmetry*, p. 355. World Scientific, Singapore, 1998.

[17] P. Meade, N. Seiberg, and D. Shih, "General Gauge Mediation", *Prog. Theor. Phys. Suppl.* **177** (2009) 143, doi:10.1143/PTPS.177.143.

[18] M. Buican, P. Meade, N. Seiberg, and D. Shih, "Exploring General Gauge Mediation", *JHEP* **0903** (2009) 016, doi:10.1088/1126-6708/2009/03/016.

[19] CMS Collaboration, "Search for supersymmetry in events with photons and missing energy", CMS Physics Analysis Summary SUS-12-018, 2012.

[20] T. A. collaboration, "Search for Diphoton Events with Large Missing Transverse Momentum in 8 TeV pp Collision Data with the ATLAS Detector",.

[21] C. Rogan, "Kinematics for new dynamics at the LHC", (2010). arXiv:1006.2727. CALT-68-2790.

[22] CMS Collaboration, "Inclusive search for squarks and gluinos in pp collisions at $\sqrt{s} = 7$ TeV", *Phys. Rev. D* **85** (2012) 012004, doi:10.1103/PhysRevD.85.012004, arXiv:1107.1279.

[23] J. Alwall, P. Schuster, and N. Toro, "Simplified models for a first characterization of new physics at the LHC", *Phys. Rev. D* **79** (2009) 075020, doi:10.1103/PhysRevD.79.075020, arXiv:0810.3921.

[24] J. Alwall, M.-P. Le, M. Lisanti, and J. G. Wacker, "Model independent jets plus missing energy searches", *Phys. Rev. D* **79** (2009) 015005, doi:10.1103/PhysRevD.79.015005, arXiv:0809.3264.

[25] D. S. Alves, E. Izaguirre, and J. G. Wacker, "Where the sidewalk ends: jets and missing energy search strategies for the 7 TeV LHC", *JHEP* **10** (2011) 012, doi:10.1007/JHEP10(2011)012, arXiv:1102.5338.

[26] LHC New Physics Working Group Collaboration, "Simplified models for LHC new physics searches", *J. Phys. G* **39** (2012) 105005, doi:10.1088/0954-3899/39/10/105005, arXiv:1105.2838.

[27] CMS Collaboration, "Updated measurements of the Higgs Boson at 125 GeV in the two photon decay channel", CMS Physics Analysis Summary HIG-13-001, 2013.

[28] CMS Collaboration, "Commissioning of the Particle-Flow reconstruction in Minimum-Bias and Jet Events from pp Collisions at 7 TeV", CMS Physics Analysis Summary PFT-10-002, 2010.

[29] CMS Collaboration, "Isolated Photon Reconstruction and Identification at sqrts", CMS Physics Analysis Summary EGM-10-006, 2011.

[30] M. Cacciari, G. P. Salam, and G. Soyez, "The Anti-k(t) jet clustering algorithm", *JHEP* **0804** (2008) 063, doi:10.1088/1126-6708/2008/04/063, arXiv:0802.1189.

[31] M. Cacciari, G. P. Salam, and G. Soyez, "FastJet User Manual", *Eur.Phys.J.* **C72** (2012) 1896, doi:10.1140/epjc/s10052-012-1896-2, arXiv:1111.6097.

[32] S. Hoeche et al., "Matching parton showers and matrix elements", (2006). arXiv:hep-ph/0602031.

[33] CMS Collaboration, "The fast simulation of the CMS detector at LHC", *J. Phys. Conf. Ser.* **331** (2011) 032049, doi:10.1088/1742-6596/331/3/032049.

[34] W. Beenakker, R. Höpker, M. Spira, and P. M. Zerwas, "Squark and gluino production at hadron colliders", *Nucl. Phys. B* **492** (1997) 51, doi:10.1016/S0550-3213(97)80027-2, arXiv:hep-ph/9610490.

[35] A. Kulesza and L. Motyka, "Threshold resummation for squark-antisquark and gluino-pair production at the LHC", *Phys. Rev. Lett.* **102** (2009) 111802, doi:10.1103/PhysRevLett.102.111802, arXiv:0807.2405.

[36] A. Kulesza and L. Motyka, "Soft gluon resummation for the production of gluino-gluino and squark-antisquark pairs at the LHC", *Phys. Rev. D* **80** (2009) 095004, doi:10.1103/PhysRevD.80.095004, arXiv:0905.4749.

[37] W. Beenakker et al., "Soft-gluon resummation for squark and gluino hadroproduction", *JHEP* **12** (2009) 041, doi:10.1088/1126-6708/2009/12/041, arXiv:0909.4418.

[38] W. Beenakker et al., "Squark and gluino hadroproduction", *Int.J.Mod.Phys. A* **26** (2011) 2637, doi:10.1142/S0217751X11053560, arXiv:1105.1110.

[39] M. Krämer et al., "Supersymmetry production cross sections in pp collisions at $\sqrt{s} = 7$ TeV", (2012). arXiv:1206.2892.

[40] CMS and ATLAS Collaboration Collaboration, "Procedure for the LHC Higgs boson search combination in Summer 2011 ", CMS Physics Analysis Summary CMS-NOTE-2011-005, 2011.

A Signal Selection Event Yields

Cut	T5gg [GeV] $m_{\tilde{g}} = 1350$ $m_{\tilde{\chi}_1^0} = 75$	T5gg [GeV] $m_{\tilde{g}} = 1350$ $m_{\tilde{\chi}_1^0} = 375$	T5gg [GeV] $m_{\tilde{g}} = 1350$ $m_{\tilde{\chi}_1^0} = 1275$	GGM [GeV] $m_{\tilde{q}} = 2000$ $m_{\tilde{g}} = 1320$	GGM [GeV] $m_{\tilde{q}} = 1500$ $m_{\tilde{g}} = 2020$
None	25.6 ± 0.3	25.6 ± 0.3	25.6 ± 0.3	33.7 ± 0.3	24.0 ± 0.2
2 $\gamma\gamma$	12.6 ± 0.2	14.7 ± 0.2	16.5 ± 0.2	12.6 ± 0.2	11.7 ± 0.2
1 loose jet	12.4 ± 0.2	14.4 ± 0.2	15.3 ± 0.2	12.2 ± 0.2	11.4 ± 0.2
Baseline Razor	11.4 ± 0.2	13.8 ± 0.2	15.1 ± 0.2	11.6 ± 0.2	10.9 ± 0.2
Signal Region	10.0 ± 0.2	12.6 ± 0.2	14.9 ± 0.2	10.6 ± 0.2	10.2 ± 0.2
$M_R > 1.5$ TeV	7.9 ± 0.1	9.6 ± 0.2	9.6 ± 0.2	7.6 ± 0.2	8.8 ± 0.1
$R^2 > 0.04$	5.5 ± 0.1	7.3 ± 0.1	9.0 ± 0.2	5.6 ± 0.1	7.2 ± 0.1

Figure 7: An example signal event yield for 19.7 fb^{-1} is shown for three T5gg mass points and two GGM mass points. The points are selected to be near the exclusion limit. The baseline razor selection includes $M_R > 600$ GeV and $R^2 > 0.01$. The signal region additionally requires $R^2 > 0.02$. All errors are statistical and all masses are in GeV.

Displaced Jet Tagging in Run 2 Data

A search for long-lived beyond the Standard Model physics is proposed to include a number of final states and models. To be precise, the long-lived particles must decay at a position measurably "displaced" from the initial interaction point. Motivated by split supersymmetry's characteristically long-lived gluinos and a variety of hidden valley models with long-lived neutral particles, these displaced signals have little to no Standard Model background. The analysis will constrain a number of beyond the Standard Model physics scenarios by developing categories of displaced jet tags similar to strategies used in b quark identification.

Split-Susy and Naturalness at the LHC

The expectation of discovering supersymmetry (SUSY) at the TeV scale has been largely motivated by arguments based on naturalness. Since the mass of the Standard Model Higgs boson is sensitive to the high energy scale where SUSY is broken (m_{SUSY}), its mass, of order the electroweak scale, ($m_h \approx m_{EW} \ll m_{SUSY}$) would need to be tuned to order m_{EW}^2/m_{SUSY}^2. To avoid fine-tuning, we would like $m_h^2 \approx m_{SUSY}^2 \implies m_{SUSY} \leq 1$ TeV. More specifically, knowing $m_H \approx 125$ GeV we expect light SUSY partners (in particular, light stops) near $\lesssim 1$ TeV to stabilize the quadratic divergences of 1 loop corrections to the Higgs mass [1]. Unfortunately these scalar partners have yet to be discovered.

It is important to note that the stability of the Higgs boson mass is not the only fine-tuning problem in particle physics. When the same argument is made for the cosmological constant we arrive at $\Lambda \geq m_{SUSY}^4$, where experimentally $\Lambda = 10^{-59}$ TeV^4. If we use the same SUSY scale as we did for the Higgs mass, $m_{SUSY} = 1$ TeV we have a new fine tuning problem of 10^{60}.

As addressed by Arkani-Hamed and Dimopoulos [2], many theoretical approaches have been motivated by a natural explanation for the Higgs mass while separately seeking an explanation of the cosmological constant through some other mechanism. Arkani-Hamed and Dimopoulos propose a reconsideration of naturalness, entertaining the idea that fine tuning could have a role to play in beyond the Standard Model physics. Conceivably, both Λ and m_h fine tuning could be resolved by the same mechanism. This un-natural model was further investigated by Giudice and Romanino [3] and dubbed "split supersymmetry".

Split SUSY assumes a much higher SUSY scale $m_{SUSY}^2 \gg 1$ TeV where all scalars (excluding the Higgs) become very heavy $O(m_{SUSY})$ and the lightest sparticles (Higgsinos and gluinos) are kept at the TeV scale by requiring the lightest neutralino to be a good dark matter candidate.

Because the scalars are so much heavier, the decay of gluinos through squarks is suppressed. The characteristic signature of split supersymmetry is thus long-lived gluinos; such processes with long lifetimes are rare in the SM.

Outlook

As the Higgs at 125 GeV has been the only scalar discovered in the LHC's $\sqrt{s} = 7$ and 8 TeV program, the natural SUSY parameter space has become more tightly constrained. If no new scalar superpartners are found at $\sqrt{s} = 13$ TeV, less natural scenarios like split SUSY would become even stronger candidates for beyond the Standard Model physics. CMS is well prepared for most, if not all, SUSY final states with prompt decays. This analysis aims to fill in the complementary parameter space not explored by current long-lived searches by analyzing underlying event kinematics in categories in displaced jet tags.

Triggering in Run 2 Data

Currently two triggers targeting displaced jet signatures are implemented in the CMS high level trigger (HLT) menu, both seeded from `L1_HTT175`. Due to the L1 H_T in-efficiency at it's nominal threshold, we are constrained to at least a cut of $H_T > 350$ GeV at the high level trigger.

- `HLT_HT350_DisplacedDijet80_DisplacedTrack`
- `HLT_HT650_DisplacedDijet80_Inclusive`

Both triggers consist of an H_T requirement (the scalar sum of the transverse momentum of jets within the tracker acceptance), two calorimeter based jets with $p_t > 80$ GeV and requirements on the tracks matched to both jets. To enforce the tracking requirements we require the jets to be central $|\eta| < 2.0$. For both paths, the jets are required to have at most 2 "prompt" tracks. For the displaced track trigger, we additionally require a track matched to the jet with high transverse displacement significance (2 dimensional impact parameter (IP) significance) with at least a transverse displacement of 0.05 cm. The significance is determined as the transverse track displacement L_{xy} divided by the error on the measurement. The displaced track trigger utilizes a special iteration of tracking designed to reconstruct tracks with 3D impact parameters as high as 20 cm.

Due to tight rate constraints in the CMS High Level Trigger menu, the two trigger strategy is employed to be as inclusive as possible to differing signal scenarios. When the signal events occur beyond the $H_T = 650$ GeV kinematic threshold, the inclusive trigger is most effective. The farther the long lived particle decays from the beam line, the better the inclusive trigger performs relative to the displaced track trigger, which needs to reconstruct a displaced track. The displaced track trigger has relatively better performance below the $H_T = 650$ GeV threshold, but is insensitive to Higgs related signatures where the higgs decays to two long lived neutral X's.

To target higgs portal processes where $H \rightarrow XX$ `L1_TripleJet_92_76_64_VBF` seeded triggers are currently being developed and studied:

- `HLT_VBF_HadronJet40`
- `HLT_VBF_DisplacedJet40`

Both triggers require two back to back jets with high eta separation and a minimum invariant mass (to match the VBF condition) and a single jet with $p_t > 40$ GeV with at most 2 prompt tracks. The hadron jet trigger is designed for decays with long life-times which occur inside the hadron calorimeter by requiring a high hadronic energy fraction of the jet. It is important to note that this signature is difficult to distinguish from noise in the hadronic calorimeter. It is possible that significant contributions to the rate would come from noise, and this contribution would need to be measured separately. The displaced jet trigger track requirements are the same as the displaced dijet track trigger above, requiring a single track of high IP significance. As before, the displaced jet trigger would target shorter lifetimes.

Displaced Jet Tags

The focus of the analysis will be defining displaced jet tags capable of targeting a variety of long lived signatures. The generation of these sequences will closely mirror those of b quark identification algorithms. The goal will be to design the identification sequence in such a way that the b-tagging community can provide insight and other displaced analyses can reuse the software.

As the characteristics of a displaced jet and its associated tracks can vary significantly with the associated physics we will generate discriminants based on generic characteristics of the calorimeter based jets:

- Number of matched prompt tracks and their IP significance
- Number of matched displaced tracks and their IP significance
- Clustering of displaced track impact parameters
- Secondary vertices reconstructed within a jet and the associated displacement
- Hadronic energy fraction (for decays inside the hadronic calorimeter)
- Muons stubs matching the jet from heavy flavor quark decays
- Missing Energy in the event

For a given category of signal, a sub-set of these quantities would be combined into a single discriminant (possibly utilizing multi-variate techniques). Examples:

- Short Lifetimes: Displaced tracks, a reconstructed secondary vertex, and high IP significance. This would be the most similar to b-tagging and likely the highest discrimination power for decays still within the pixel layers.
- Long Lifetimes: In the regime where we cannot reliably reconstruct the displaced tracks we would ask for small numbers of prompt tracks. Lacking a secondary vertex we could regain sensitivity by using muon stubs from heavy flavor decays.
- Hadron Calorimeter decays: When we do not expect any tracks we require high hadronic energy fraction and small numbers of prompt tracks. Again, looking for muon stubs could be beneficial.
- Singly Produced: Long lived particles are not always pair produced. In some scenarios, a long lived particle (that would decay in the detector) and a “WIMP-y” hidden sector particle (that would not decay in the detector) are produced. This topology would have displaced jets and missing energy. The missing energy in the event could be used as a discriminator for this variety of jet.

Discovery Motivated Analysis

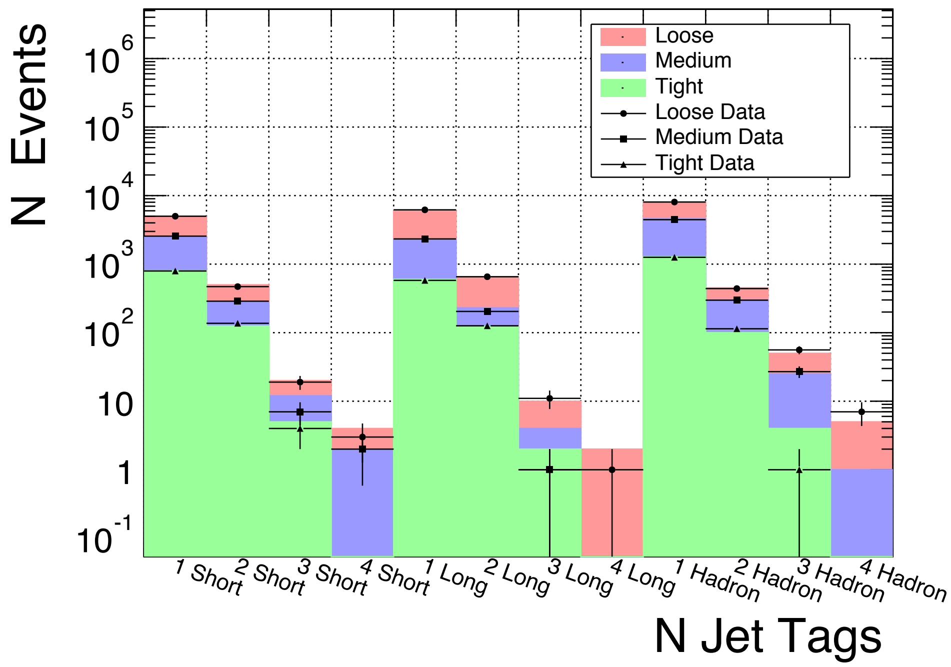

Figure 1: An example background prediction made in categories of displacement and varied working points.

One of the most important aspects of displaced jet analysis, is how visibly striking the signature can be. This is especially the case for decays within the tracker. If we are able to reject enough QCD events and detector effects to narrow the selected number of events, we could look through the event displays by hand. In many scenarios the events would be self-diagnostic.

The coarse level of the analysis will be performed in loose, medium, and tight working points for each of the categories (Figure 1). These distributions would give an inclusive view of possible displaced physics, and point us in directions to review event displays.

It is a goal to perform the background estimation with limited dependence on the trigger path (such as the ABCD approach). In this way, we could run the analysis over multiple primary datasets in search of displaced physics. For instance, by looking at the single electron and single muon datasets would give sensitivity to associated higgs production where the higgs is coupled to a hidden sector. Even though the un-seen width of the higgs would be sensitive to such a signature, the presence of displaced jets can be much more convincing.

It would also be interesting to analyze the 8 TeV parked VBF data for displaced jets. Such an analysis would likely need to wait till the end of Run 2.

References

[1] S. Dimopoulos, G. Giudice. Naturalness constraints in supersymmetric theories with non-universal soft terms, Phys. Lett. B357 (1995), no. 4, 573,

[2] N. Arkani-Hamed and Savas Dimopoulos. Supersymmetric Unification Without Low Energy Supersymmetry And Signatures for Fine-Tuning at the LHC. arXiv:hep-th/0405159v2

[3] G. Giudice, A. Romanino. Split Supersymmetry. arXiv:hep-ph/0406088v2

[4] N. Arkani-Hamed, S. Dimopolous, G.F. Giudice, A. Romanino. Aspects of Split Supersymmetry. arXiv:hep-ph/0409232v2

[5] N. Arkani-Hamed, A. Gupta, D. Kaplan, Neal Weiner, Tom Zowarski. Simply Unnatural Supersymmetry. arXiv:1212.6971v1

[6] J. Hewett, B. Lillie, M. Masip, and T. Rizzo, Signatures of long-lived gluinos in split supersymmetry. arXiv:hep-ph/0408248v1

[7] The CMS Collaboration. EXO-12-038. Search for long-lived neutral particles decaying to dijets.

[8] The CMS Collaboration. EXO-11-035. Search for long-lived particles in events with photons and missing energy in proton-proton collisions at $\sqrt{s} = 7$ TeV.

[9] The CMS Collaboration. EXO-11-067. Search for new physics with long-lived particles decaying to photons and missing energy in pp collisions at $\sqrt{s} = 7$ TeV

[10] The CMS Collaboration. EXO-12-048. Search for new physics in monojet events in pp collisions at $\sqrt{s} = 8$ TeV

[11] S. Weinberg, Phys. Rev. Lett. **59**, 2607 (1987)

Princeton University, Department of Physics Jadwin Hall, Princeton NJ 08544

E-mail address: joshuarh@princeton.edu